Solar Energy 178 (2019) 295–307

Contents lists available at ScienceDirect

Solar Energy

journal homepage: www.elsevier.com/locate/solener

Thermal analysis of geopolymer concrete walls containing microencapsulated phase change materials for building applications

Vinh Duy Cao[a,b], Shima Pilehvar[a,c], Carlos Salas-Bringas[b], Anna M. Szczotok[a,d], Tri Quang Bui[a], Manuel Carmona[d], Juan F. Rodriguez[d], Anna-Lena Kjøniksen[a,*]

[a] Faculty of Engineering, Østfold University College, N-1757 Halden, Norway
[b] Faculty of Science and Technology, Norwegian University of Life Sciences, N-1432 Ås, Norway
[c] Department of Material Engineering and Manufacturing, Technical University of Cartagena, Cartagena, Murcia, Spain
[d] Department of Chemical Engineering, University of Castilla – La Mancha, 13004 Ciudad Real, Spain

ARTICLE INFO

Keywords:
Microencapsulated phase change materials
Geopolymer concrete
Energy efficiency
Solar radiation

ABSTRACT

The potential of utilizing geopolymer concrete (GPC) walls containing microencapsulated phase change material (MPCM) in buildings at different environmental conditions has been investigated. The effect of climate conditions (temperature, solar radiation) and MPCM design (shell thickness, concentration) on the energy efficiency of buildings was systematically analyzed based on numerical calculations utilizing the finite differences method with an energy balance approach. The energy efficiency of buildings was found to increase at higher levels of MPCM addition and for thicker concrete walls. When the outdoor temperature is higher than the indoor temperature, increasing the maximum solar radiation causes a higher power consumption, a lower power reduction, and accordingly a reduced energy efficiency of the buildings. Utilizing a PCM with a melting temperature close to the average outdoor and indoor temperatures has a positive effect on enhancing the energy efficiency of buildings. Numerical calculations were used to evaluate the efficiency of using GPC containing two different types of MPCM (PS-DVB/RT27 with a paraffin Rubitherm®RT27 core and a shell of polystyrene cross-linked with divinylbenzene and MF/PCM24 with a paraffin mixture core and a melamine–formaldehyde polymer shell) at the environmental conditions of Oslo and Madrid throughout one year. It was found that a significant reduction of the annual power consumption for heating/cooling can be achieved in both Oslo and Madrid. It was also found that the wall orientation and the season have significant effects on the power consumption and power reductions. The GPC containing MPCM was found to exhibit better performance in Madrid than in Oslo. The developed model can be used as a quantitative tool to design MPCM-concrete walls in different climates.

1. Introduction

Approximately 40% of the total energy consumption is related to buildings, and a significant amount of this energy is due to heating and cooling (EU Directive 2002/91/EC; EU Directive 2010/31/UE). Accordingly, reducing the energy consumption of buildings is important for achieving the energy and climate targets of the world. Improved construction techniques and advanced material technology can significantly reduce the energy consumption needed to keep a comfortable indoor temperature.

Integration of microencapsulated phase change materials (MPCM) into building materials has been investigated to create materials with a high thermal energy storage capacity (Borreguero et al., 2014; Cao et al., 2018b, 2017; Cui et al., 2018; Eddhahak-Ouni et al., 2014; Hunger et al., 2009 ; Pilehvar et al., 2017b; Pisello et al., 2017; Ramakrishnan et al., 2017a,b,c; Shadnia et al., 2015; Wei et al., 2017). Phase change materials are materials that can store and release high amounts of thermal energy, utilizing the phase transition of the materials. The main parameters that influence the storage and release of thermal energy are the heat storage capacity, the thermal conductivity, the melting temperature of the PCM, and the outdoor environment. Incorporating MPCM into a building material is expected to improve the thermal energy storage capacity, resulting in higher energy efficiency and reduced power consumption for heating and cooling. Another advantage of utilizing PCM in building materials is the possibility of moving the maximum thermal load of the buildings to periods where the electricity demand is low (e.g., at night), thereby reducing the peak electricity demand.

* Corresponding author.
E-mail address: anna.l.kjoniksen@hiof.no (A.-L. Kjøniksen).

https://doi.org/10.1016/j.solener.2018.12.039
Received 2 May 2018; Received in revised form 3 December 2018; Accepted 17 December 2018

Nomenclature

C_p	specific heat capacity, J/Kg °C
q_s“	solar radiation, W/m^2
T	temperature, °C
t	time, s
h_i	indoor heat transfer coefficient, W/m^2 °C
h_o	outdoor heat transfer coefficient, W/m^2 °C
P	power consumption, kWh/m^2
Pr	power reduction, %
k	thermal conductivity, W/m °C
$Q_{convection}$	convective heat transfer, W/m^2
Q_{rad}	radiative heat transfer, W/m^2

Greek symbols

φ	heat flux, W/m^2
α_s	absorptivity of the outdoor wall surface
ε	emissivity of the outdoor wall surface
σ	Stefan–Boltzmann constant, W/m^2·K^4
ρ	density, Kg/m^3

Subscripts

sky	average sky temperature
i	discretized node
m	interior discretized node
room	room temperature
ave	average
out	outdoor temperature
max	maximum temperature
min	minimum temperature
con	concrete
MPCM-con	concrete containing MPCM

Abbreviations

MPCM	microencapsulated phase change materials
PCC	Portland cement concrete
GPC	geopolymer concrete

Concrete-based materials are among the most used materials for buildings. This is due to their high mechanical strength and the possibility of changing the properties by varying the concrete recipe. Concrete has a moderate thermal energy storage capacity, which can be improved by integration of MPCM (Cao et al., 2017; Cui et al., 2018; Hunger et al., 2009; Pilehvar et al., 2017b; Wei et al., 2017). The enhancement of the thermal energy storage capacity of concrete will improve the energy efficiency of buildings.

Experimental studies of the thermal response of concrete walls containing MPCM show very promising results regarding saving building energy consumption (Cao et al., 2017, 2018c; Hunger et al., 2009). However, experimental studies are usually costly and time consuming, especially when it is desirable to compare a range of potential designs to evaluate their respective performance. Alternatively, simulation studies are able to determine the efficiency of a design without physically building the systems. This significantly reduces the investigation time and the overall cost of building the system. Due to the benefit of numerical models, some numerical methods have been developed to simulate the thermal impact of building materials containing PCM/MPCM (Al-Saadi and Zhai, 2013; Biswas and Abhari, 2014; Borreguero et al., 2011; Darkwa and Su, 2012; Diaconu and Cruceru, 2010; Gowreesunker et al., 2012; Lamberg et al., 2004; Marin et al., 2016; Thiele et al., 2015; Xie et al., 2018; Zwanzig et al., 2013). The heat capacity method is one of the most commonly used numerical methods, and show good agreement with experimental data (Borreguero et al., 2011; Lamberg et al., 2004). Nevertheless, while the building materials containing PCM/MPCM exhibit an asymmetric melting area (Cao et al., 2017; Cui et al., 2015; Joulin et al., 2014; Lachheba et al., 2015), most studies define C_p(T) as a piecewise function of temperature (Lamberg et al., 2004; Thiele et al., 2015) or a Gaussian function of temperature (Diaconu and Cruceru, 2010), which assume that the melting area is symmetric. A mismatch between the model and realistic conditions induces inaccuracies in the models.

Few studies have numerically calculated the energy consumption of a building over an entire year in different cities to explore the role of various seasons on the thermal impact of building materials containing PCM/MPCM (Biswas and Abhari, 2014; Diaconu and Cruceru, 2010; Xie et al., 2018; Zwanzig et al., 2013). There are conflictive observations regarding seasonal variations of the energy efficiency of buildings utilizing PCM/MPCM. Some studies found that the energy reduction in the summer was higher than in the winter (Biswas and Abhari, 2014; Zwanzig et al., 2013) while other studies came to the opposite conclusion (Diaconu and Cruceru, 2010). The discrepancies could be due to different climate conditions with dissimilarities in solar radiation and outdoor temperatures. However, further investigations are required to present clear evidence on how the seasons and climates can affect the thermal impact of concrete containing MPCM.

Ordinary Portland cement concrete is one of the major building materials worldwide, and has been studied for incorporation of microencapsulated phase change materials (Cui et al., 2015; Joulin et al., 2014; Hunger et al., 2009). However, the high amount of CO_2 emission from production of Portland cement is a major drawback (Benhelal et al., 2013). Approximately 5–7% of global man-made CO_2 emissions are due to Portland cement production (Sumesh et al., 2017; Turner and Collins, 2013). It has been estimated that the CO_2 emission from geopolymer concrete is 9% lower than for Portland cement concrete (Turner and Collins, 2013). However, the calculations were based on a geopolymer concrete that was heated to 60–80 °C during curing. Curing the geopolymer concrete at ambient conditions (Pilehvar et al., 2018; Pilehvar et al., 2017a) reduces the CO_2 emissions with 21% compared to Portland cement concrete. Geopolymer concrete exhibit improved compressive strength compared to Portland cement concrete, (Pilehvar et al., 2018; Pilehvar et al., 2017a) and have been shown to have a better resistance to high temperatures (Kong and Sanjayan, 2010) and fire (Sarker et al., 2014), smaller drying shrinkage (Olivia and Nikraz, 2012), as well as superior acid (Bakharev, 2005) and salt water (Olivia and Nikraz, 2012) resistance. The geopolymer binder is synthesized by mixing materials rich in silica and amorphous alumina with a strong alkaline activator (Part et al., 2015; Singh et al., 2015). A high proportion of industrial by-products such as fly ash, coal ash, and blast furnace slag are often used in geopolymer concrete. Therefore, an environmentally friendly geopolymer concrete (GPC) with low CO_2 emission was selected for this work.

The objective of the present work is to numerically investigate how the variation of different climate conditions influence the thermal impact of buildings utilizing concrete walls containing microencapsulated phase change materials.

A mathematical model was developed to simulate the effect of MPCM addition on the thermal performance of buildings. In addition, the heat capacity as function of temperature for concrete containing microencapsulated phase change materials was utilized in the numerical model. The effect on the energy efficiency of buildings of MPCM type and concentration, the thickness of the concrete walls, solar radiation, and outdoor temperature was investigated. The possibility of utilizing concrete containing MPCM walls at the climate conditions of Oslo and Madrid over a span of one year was evaluated with special

attention on the effect of wall orientation and seasons. The main purpose is to explore the combined effect of different climates conditions such as solar radiation and outdoor temperature on the energy efficiency of MPCM addition.

2. Experimental

2.1. Materials

Geopolymer concrete containing microencapsulated phase change materials (MPCM-GPC) was fabricated by mixing class F fly ash (FA), ground granulated blast furnace slag (GGBFS), sand, aggregates, retarder, an alkaline activator solution and MPCM. Table 2 summarizes the composition of geopolymer concrete containing MPCM (MPCM-GPC) (Pilehvar et al., 2018; Pilehvar et al., 2017b). MPCM was incorporated into GPC at 0, 2.6 and 5.2 wt%. The concentration of MPCM was limited to 5.2 wt% since higher concentrations of MPCM resulted in too low workability of the geopolymer concrete.

Two different kinds of microcapsules were utilized. PS-DVB/RT27 microcapsules consists of a paraffin Rubitherm®RT27 core coated with a PS-DVB (polystyrene cross-linked with divinylbenzene) shell. This MPCM was prepared by a polymerization suspension process in our lab. For more information about the fabrication process of PS-DVB/RT27, see Szczotok et al. (2017). The commercial Microtek microcapsules, MPCM24D (MF/PCM24) have a paraffin core and a melamine-formaldehyde polymer shell (MF). The MPCM properties are summarized in Table 1.

The concrete samples containing 0 wt%, 2.6 wt% and 5.2 wt% of MPCM were named GPC0, GPC-2.6-X and GPC-5.2-X, respectively. X is the name of integrated MPCM (PS-DVB/RT27 or MF/PCM24).

Sand (density of 2.7 g/cm^3) and aggregates (density of 2.6 g/cm^3) were supplied by Gunnar Holth and Skolt Pukkverk AS, Norway. In addition, the class F fly ash (density = 2.26 ± 0.02 g/cm^3) and ground granulated blast furnace slag (GGBFS) (density = 2.85 ± 0.02 g/cm^3) was purchased from Norcem, Germany and Cemex, Germany, respectively.

The alkaline activator solution consists of a mixture of a sodium silicate solution (density = 1.93 g/cm^3, 35 wt% solids consisting of 27 wt% of SiO_2 and 8 wt% of Na_2O) and a 14 M NaOH (560 g/L) solution. The ratio between the sodium silicate solution and NaOH(aq) is 1.5 (Pilehvar et al., 2018). For the current recipe, $m_{Na2SiO3(aq)}$ = 120 g, and $m_{NaOH(aq)}$ = 80 g. The sodium silicate solution has a molar ratio of SiO_2 to Na_2O of 3.49 and viscosity of 0.1 Pa·s at 20 °C. In order to improve the workability as well as the mixing ability of MPCM into GPC, a naphthalene based retarder (density of 1.2 g/cm^3; FLUBE OS 39, Bozzetto Group, Italy) was selected (Jang et al., 2014; Nematollahi and Sanjayan, 2014a,b; Pilehvar et al., 2018).

The thermal properties of GPC containing various concentrations of MPCM were determined by a home-made guarded hot plate system (Cao et al., 2018a). The thermal properties are summarized in Table 3 and Table 4. For more information regarding the guarded hot plate system and the determination of the thermal properties, see Cao et al. (2017 and 2018a).

The specific heat capacity as a function of temperature of GPC containing microcapsules can be described by (Cao et al., 2018a):

$$Cp(T) = \begin{cases} Cp_o + h * \dfrac{w_l^{2m_l}}{\left(w_l^2 + \left(2^{\frac{1}{m_l}} - 1\right) * (2T - 2T_m)^2\right)^{m_l}} & for \quad T \le T_m \\ Cp_o + h * \dfrac{w_r^{2m_r}}{\left(w_r^2 + \left(2^{\frac{1}{m_r}} - 1\right) * (2T - 2T_m)^2\right)^{m_r}} & for \quad T > T_m \end{cases} \tag{1}$$

where T_m is the melting temperature of phase change materials. w_l and w_r are the phase change temperature range on the left side and right side of the melting peak, respectively. m_l and m_r are shape parameters for the left and right side of the peak, respectively. Cp_o and h are respectively the specific heat capacity outside the melting range and the height of the melting peak. For more information about the Cp(T) fitting process, see Cao et al. (2018a).

2.2. Numerical method

The effect of MPCM addition on the thermal performance of concrete walls was numerically evaluated. The indoor surface temperature reduction, the time delay of the maximum thermal load, the power consumption, and the power reduction for the heating and cooling system were calculated based on a simplified, uninsulated concrete wall and a constant indoor temperature.

Fig. 1 shows the model used to investigate the thermal behavior of the concrete walls. The following assumptions of the material properties and environmental conditions were made to simplify the calculation process:

- The thickness of the concrete wall is significantly smaller than the other dimensions. Therefore, the heat transfer process across the concrete walls is assumed as a one-dimensional problem.
- The MPCM concrete sample is homogeneous and isotropic.
- There is no heat generation in the concrete samples.
- The convection effect in the melted PCM is omitted.
- The convection coefficients for the indoor and outdoor environment are assumed to be constant.
- The heat from people and devices are neglected.

Based on these assumptions, the equation for one-dimensional heat transfer across the MPCM-concrete wall is (Cengel, 2002; Lamberg et al., 2004; Thiele et al., 2015):

$$k\frac{\partial^2 T}{\partial x^2} = \rho C_p(T)\frac{\partial T}{\partial t} \tag{2}$$

where k, ρ, x are the thermal conductivity, density, and thickness of the wall, respectively. $C_p(T)$ is the specific heat capacity as a function of temperature of GPC containing microcapsules and can be described by Eq. (1).

In order to solve the model, the finite difference method was selected due to its high accuracy and fast computation (Özişik et al., 2017). The finite difference method has 3 different schemes: the explicit scheme, the fully implicit scheme, and the Crank-Nicolson scheme (semi-implicit scheme). While the explicit scheme requires small time steps to obtain stable data, the fully implicit scheme (first order in time) and Crank–Nicolson scheme (second order in time) works well and provides high accuracy for large time steps (Özişik et al., 2017). Although the Crank-Nicolson scheme shows highest accuracy, it can contain spurious oscillations especially when the time step is large

Table 1
The properties of the microencapsulated phase change materials.

MPCM name	Size (μm)		T_{melt} (°C)	ΔH (J/g)	Reference
	Single	Aggregates (mean size)			
PS-DVB/RT27	10–100	130	24.9	100	Szczotok et al. (2017)
MF/PCM24	10–30	21	21.9	154	Cao et al. (2018c)

Table 2
Composition of Geopolymer concrete.

MPCM (wt%)	Alkaline solution (g)	Water (g)	FA* (g)	GGBFS** (g)	Sand (g)	Aggregate (g)	Retarder (g)	MPCM (g)
0	200	50	300	200	871.2	851.7	5	0
2.6					696.9			63
5.2					522.7			117

* FA: Flyash.
** GGBFS: Ground granulated blast-furnace slag.

Table 3
Summarization of the thermal properties of GPC containing PS-DVB/RT27 (Cao et al., 2018a).

MPCM (%)	k (W/m °C)	C_p (J/Kg °C)							ρ (Kg/m^3)
		Cp_o	h	w_l	w_r	m_l	m_r	T_m	
0	1.35	891	–	–	–	–	–	–	2199
2.6	1.13	960	199	9.0	3.3	159	275	23.3	2057
5.2	0.87	1062	568	7.8	2.3	1.7	3.4	25.3	1960

Table 4
Summarization of the thermal properties of GPC containing MF/PCM24 (Cao et al., 2018a).

MPCM (%)	k (W/m °C)	C_p (J/Kg °C)							ρ (Kg/m^3)
		Cp_o	h	w_l	w_r	m_l	m_r	T_m	
0	1.35	891	–	–	–	–	–	–	2199
2.6	1.02	982	404	5.6	1.6	1.3	2.8	23	2023
5.2	0.74	1125	851	6.3	2.9	1.4	5.3	23.7	1875

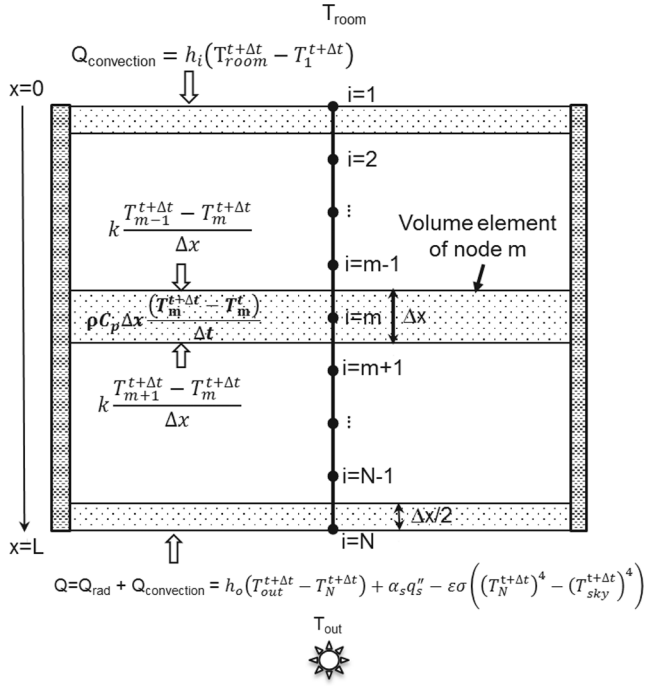

Fig. 1. Schematic representation of the MPCM-concrete wall, and finite differences method using the energy balance approach with boundary conditions. The energy balance states that heat transferred into the volume element (Q) from all of its surfaces is equal to the change in the energy content of the volume element ($\Delta E_{element}$) during Δt (Cengel, 2002).

(Khoshghalb et al., 2011). The fully implicit scheme was therefore employed to achieve good accuracy without oscillations for the yearly numerical calculations at reduced computing times.

For the current work, the fully implicit finite difference method using the energy balance approach, which was successfully applied by other research groups (Ascione et al., 2014; Cengel, 2002; Ramakrishnan et al., 2017d,e), will be employed to solve the model in order to predict the annual thermal performance of building utilizing geopolymer concrete containing microcapsules. This method is based on discretizing the medium into a number of nodes where the distance (thickness) between two adjacent nodes is Δx. The volume elements over the nodes, where energy balance is applied, are formed to determine the temperatures at all nodes of the sample (Fig. 1).

In addition, boundary conditions were applied to solve Eq. (2):

- Interior node i = 1 (x = 0, indoor wall surface) (boundary condition (Cengel, 2002)): For the room, a constant indoor temperature T_{room} is maintained at 23 °C by a HVAC (heating, ventilation and air conditioning) system. Only the convective heat transfer is imposed at the interior wall surface while the radiative heat transfer due to the different temperature between the indoor wall surface and the room temperature is neglected.

$$k\frac{T_2^{t+\Delta t}-T_1^{t+\Delta t}}{\Delta x}+h_i(T_{room}^{t+\Delta t}-T_1^{t+1\Delta t})=\rho C_p(T)\frac{\Delta x}{2}\frac{(T_1^{t+\Delta t}-T_1^{t})}{\Delta t} \quad (3)$$

- Inner node i = 2 to i = N − 1

$$k\frac{T_{m-1}^{t+\Delta t}-T_m^{t+\Delta t}}{\Delta x}+k\frac{T_{m+1}^{t+\Delta t}-T_m^{t+\Delta t}}{\Delta x}=\rho C_p(T)\Delta x\frac{T_m^{t+\Delta t}-T_m^{t}}{\Delta t} \quad (4)$$

- Exterior node i = N (x = L, outdoor wall surface) (boundary condition (Pasupathy et al., 2008; Cengel, 2002; Diaconu and Cruceru, 2010; Thiele et al., 2015)): the exterior wall surface is subjected to a time dependent outdoor temperature (T_{out}) and a time dependent solar radiation heat flux (q″$_s$). The combined convective and radiative heat transfer is imposed at the exterior wall surface.

$$k\frac{T_{N-1}^{t+\Delta t}-T_N^{t+\Delta t}}{\Delta x}+h_o(T_{out}^{t+\Delta t}-T_N^{t+\Delta t})+\alpha_s q_s''-\varepsilon\sigma((T_N^{t+\Delta t})^4-(T_{sky}^{t+\Delta t})^4)$$
$$=\rho C_p(T)\frac{\Delta x}{2}\frac{(T_N^{t+\Delta t}-T_N^{t})}{\Delta t} \quad (5)$$

Different values of Δt and Δx were tested to determine values for the simulation where the simulated data is stable and there is no difference when the values of Δt and Δx are changed. Based on this test, Δt = 60 s and Δx = 0.005 m were used. The temperature dependent specific heat capacity Cp(T) is updated at every iteration according to Eq. (1). The initial temperature of the system was set as 23 °C.

T_{out}, T_{sky} and T_N represent the outdoor temperature, the average sky temperature and the outdoor wall surface temperature (x = L), σ is the Stefan–Boltzmann constant, α_s and ε are the total absorptivity and emissivity of the outdoor wall surface, respectively (Kreith et al., 2012; Thiele et al., 2015). The indoor heat transfer coefficient h_i was set to 8 W/m^2 K while the outdoor heat transfer coefficient h_o was set to 20 W/m^2 K. These values are similar to the values recommended by ASHRAE (ASHRAE, 2013), and has been utilized for similar calculations previously (Al-Sanea, 2002; Alawadhi, 2008; Thiele et al., 2015). The total hemispherical solar absorptivity and surface emissivity of the outdoor wall surface were 0.65 and 0.87, respectively (Kreith et al.,

2012). An average sky temperature $T_{sky} = (T_{out} - 12)$ °C was used (Al-Sanea, 2002; Garg, 1982).

The above equations for all nodes was programmed and solved in MATLAB (Mathworks Inc., Natick, MA, USA). The indoor surface temperature ($T_{x=0}$), and the heat flux on the indoor surface (φ_{indoor}) was calculated:

$$\varphi_{indoor}(t) = h_i(T^t_{room} - T^t_1) \quad (6)$$

- **Energy efficiency of MPCM addition under various simulated environmental conditions**

In the simulations, the outer wall surface of the concrete wall was exposed to a sinusoidal outdoor temperature variation (Eq. (9)) and solar radiation (Eq. (8)) while the indoor room temperature was kept constant at 23 °C. The effect of MPCM concentration, wall thickness, the maximum solar radiation and the average outdoor temperature on the power consumption, power reduction and delay time of the maximum thermal load were numerically investigated. In order to achieve a steady state, simulations were run for 4 cycles (days) of varying outdoor temperatures and solar radiation, the temperature and heat flux for the third day were determined.

The power needed for a heating/cooling system to keep the indoor temperature stable was determined as:

$$P = \frac{\int_0^{24h} |\varphi_{indoor}|\ dt}{3600 \cdot 10^3} \quad (7)$$

The power reduction Pr is:

$$Pr = \frac{P_{Con} - P_{MPCM-Con}}{P_{Con}} \cdot 100\% \quad (8)$$

where P_{Con} and $P_{MPCM\text{-}Con}$ are the power consumption of a heating and cooling system working within one day, for concrete without MPCM and with MPCM, respectively.

o **MPCM concentration**

The MPCM concentration was varied to evaluate effect on the thermal performance of concrete. Accordingly, three MPCM concentrations of 0, 2.6 and 5.2 wt% MPCM per solid of content of concrete were selected. The concentration of MPCM was limited to 5.2 wt% since higher concentrations of MPCM resulted in too low workability of the concrete.

o **Concrete thickness**

The thickness of the concrete wall affects the heat transfer process, and is therefore important for the thermal performance of buildings. The thickness of the concrete walls was varied from 5 to 15 cm to investigate the effect on the thermal performance.

o **Solar radiation**

The time dependent solar radiation heat flux q''_s which mimics maximum solar radiation conditions during summer time (July) of the city of Madrid, Spain (Pérez-Burgos et al., 2014) was utilized:

$$q''_s = \begin{cases} 0 & for\ \ 21{:}00 \le t \le 5{:}00 \\ q''_{s,max}\sin\left(\frac{\pi}{57600}t - \frac{5\pi}{16}\right) & for\ \ 5{:}00 < t < 21{:}00 \end{cases} \quad (9)$$

where $q''_{s,max}$ is the maximum daily solar radiation heat flux. In this article, the maximum daily solar radiation heat flux was varied from 0–1000 W/m^2 in steps of 250 W/m^2 to cover European conditions during summer time. The maximum daily solar heat flux was assumed to occur at 13:00 (Pérez-Burgos et al., 2014).

o **Outdoor temperature**

To mimic outdoor conditions, the ambient outdoor temperature T_{out} was imposed as a sinusoidal function of time as:

$$T_{out}(t) = \frac{T_{max} + T_{min}}{2} + \frac{T_{max} - T_{min}}{2}\sin\left(\frac{\pi}{43200}t - \frac{2\pi}{3}\right) \quad (10)$$

where T_{max} and T_{min} are the maximum and minimum outdoor temperatures during a day, respectively. The maximum outdoor temperature T_{max} were set at 14:00. The efficiency of MPCM addition on the thermal performance of concrete buildings is strongly dependent on the interplay between the phase change temperature and the outdoor temperature. Therefore, the outdoor temperature conditions were varied to evaluate the optimal temperature conditions for the MPCM utilized in this study. An outdoor temperature variation of $(T_{max} - T_{min})/2 = 5$, 7.5 and 10 °C were utilized, and the average outdoor temperatures $(T_{max} + T_{min})/2$ was varied from 0 °C to 40 °C.

- **Evaluation of building envelopes using single wall geopolymer concrete containing MPCM at the conditions of two European cities (Oslo and Madrid).**

The possibility of utilizing the geopolymer concrete containing MPCM as a simple single wall for a single family home in the climate zones of Oslo and Madrid were evaluated. The outdoor temperature and solar radiation as function of time for a typical year in Oslo and Madrid for Eq. (1) were obtained from weather data (Climate Consultant software (energy-design-tools.aud.ucla.edu.)). The effect of wall orientation (south, east, north and west facing walls) and the season during a typical year on power consumption and power reduction were evaluated. GPC without MPCM and GPC containing 5.2 wt% of PS-DVB/RT27 and MF/PCM24 were selected for the evaluation.

The power consumption of a heating and cooling system during each season for each wall orientation is:

$$P_{n,j} = \frac{\int_{t1}^{t2} |\varphi_{indoor}|\ dt}{3600 \cdot 10^3} \quad (11)$$

where $P_{n,j}$ is the power consumption of a wall facing the *n* direction (south, east, north and west) during season j (spring, summer, autumn and winter). t1 and t2 are the initial and final time of each season. For this work, the spring, summer, autumn and winter were set as 21st March–20th June, 21st June–23rd September, 24th September–21st December and 22nd December–20th March, respectively.

Furthermore, the average power consumption through all four wall orientations of a single house was also determined:

$$P_{ave,j} = \sum \frac{P_{n,j}}{4} \quad (12)$$

3. Results and discussions

3.1. Effect of MPCM concentration

In order to explore how MPCM-concrete structures work when they are exposed to different operating conditions, numerical simulations were carried out. In the simulations, the outer wall surface of the concrete wall was exposed to a sinusoidal outdoor temperature variation (Eq. (9)) with T_{min} = 15 °C and T_{max} = 35 °C while the indoor room temperature was kept constant at 23 °C. The thickness of the concrete wall was set to 10 cm. The simulations also include solar radiation (Eq. (8)), with a maximum of 750 W/m^2, which mimics the maximum solar radiation during summer time (July) of the city of Madrid, Spain (Pérez-Burgos et al., 2014).

The effect of MPCM concentration on the simulated indoor surface temperature (Fig. 2a) and inner wall heat flux (Fig. 2b) as function of time within a 24 h period are shown in Fig. 2. The addition of MPCM

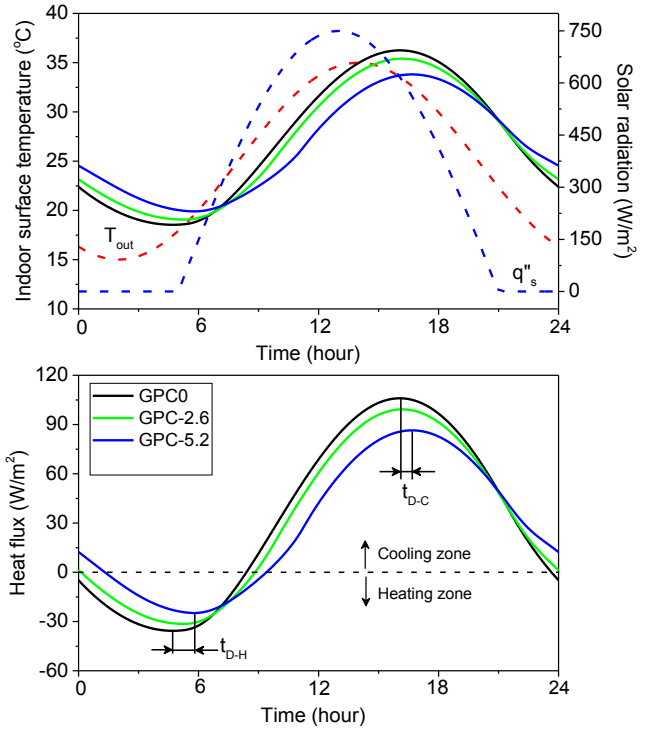

Fig. 2. (a) The simulated indoor surface temperature and (b) the simulated indoor surface heat flux through a 10 cm thick GPC containing PS-DVB/RT27 wall after exposing it to a sinusoidal outdoor temperature fluctuation (T_{out}) and maximum solar radiation (q''_s) of 750 W/m^2.

causes a slight transition point around the melting point of PCM for both the indoor surface temperature and the heat flux. This is especially evident at the highest MPCM concentration. This transition is the effect of the PCM latent heat, and is in good agreement with previous findings (Borreguero et al., 2014; Cui et al., 2015; Hunger et al., 2009).

The inclusion of MPCM in the concrete structure reduces the effect of outdoor temperature variations on the indoor surface temperature. This is due to the higher heat storage capacity and lower thermal conductivity of MPCM-concrete. The variation of the indoor surface temperature of the MPCM-concrete samples is smaller than that of concrete without MPCM, and decreases as the concentration of MPCM is increased (Fig. 2a). The maximum and minimum indoor surface temperature as a function of MPCM concentration are summarized in Fig. 3a.

In order to keep a constant indoor temperature, the total heat transfer at the indoor surface (heat gain/loss) should be compensated by a heating/cooling system. The heat gain and loss can be determined by integrating the heat flux on the indoor surface of the concrete wall (Fig. 2b). The total energy consumption for the heating/cooling system is the sum of the heating power consumption when the indoor surface temperature $T_{x=0} < T_{room}$ (heating zone), and the cooling power consumption when the indoor surface temperature $T_{x=0} > T_{room}$ (cooling zone). The total calculated power consumption (Eq. (6)) for the heating/cooling system to maintain an indoor temperature of 23 °C and the power reduction (Eq. (8)) as a function of MPCM concentration are shown in Fig. 3b.

The effect of MPCM addition on the regulation of the indoor environment can be observed by examining the indoor surface temperature. According to Fig. 3a, the maximum indoor surface temperature of MPCM-concrete decreases with approximately 3 °C while the minimum indoor surface increases with almost 1.5 °C after adding 5.2 wt% PS-DVB/RT27. This indicates that an increase of MPCM concentration results in a smaller indoor temperature variation, thereby maintaining the temperature closer to the human comfort zone. Accordingly, a lower power consumption is needed for the heating and cooling system to maintain the indoor environment at the desired temperature (Fig. 3b).

Fig. 3b shows that the power consumption to maintain the indoor

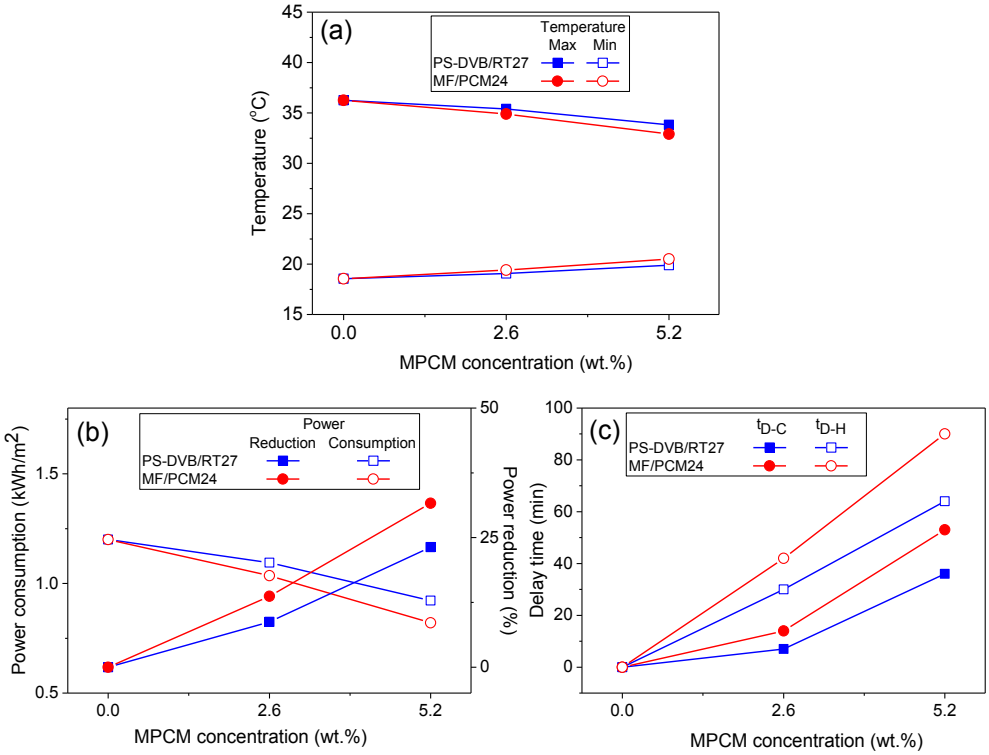

Fig. 3. (a) The maximum and minimum indoor surface temperature; (b) the power consumption and the power reduction; (c) the delay time of the maximum (t_{D-H}) and minimum (t_{D-C}) power consumption of the MPCM-concrete wall compared to GPC without MPCM as a function of MPCM concentration.

temperature at 23 °C decreases substantially with increasing MPCM concentration. The addition of 5.2 wt% PS-DVB/RT27 can reduce the power consumption with approximately 25%. This demonstrates that the utilization of MPCM will have a significant effect on the energy efficiency of buildings. The effect is not only due to the higher heat storage capacity but also due to the better insulation properties of MPCM-concrete, which is in agreement with previous experiments (Cao et al., 2017; Hunger et al., 2009) and numerical calculations (Thiele et al., 2015).

The addition of MPCM to concrete also delays the peak of the cooling (t_{D-C}) and heating loads (t_{D-H}) as shown in Fig. 2b. This effect comes from the ability of PCM to store and release a high amount of energy during the phase change in combination with the lower thermal conductivity after the addition of MPCM into concrete. As can be seen from Fig. 2b, there are two main peaks for the indoor surface heat flux: the heating peak from 03:00 to 06:00 and the cooling peak from 14:00 to18:00, depending on the amount of MPCM in the samples. They are correlated to the outdoor temperature peaks where the lowest temperature occurs at 02:00 and the highest temperature at 14:00. The effect of adding MPCM on the delay time of the power consumption peaks is shown in Fig. 3c. The delay time increases with higher MPCM concentrations, reaching approximately 65 min for the heating peak (minimum indoor surface temperature) and 40 min for the cooling peak (maximum indoor surface temperature) after adding 5.2 wt% of PS-DVB/RT27.

As can be seen in Fig. 3, geopolymer concrete containing MF/PCM24 has lower power consumption, higher power reduction and longer delay time of the heating/cooling peak than GPC containing PS-DVB/RT27. This indicates that MF/PCM24 has a greater thermal impact on GPC compared to PS-DVB/RT27. This is probably caused by the higher heat storage capacity of MF/PCM24 compared to PS-DVB/RT27 (Table 1), and the lower thermal conductivity of GPC containing MF/PCM24 (Tables 3 and 4)

3.2. Effect of solar radiation

In order to evaluate the effect of solar radiation on the energy efficiency of MPCM-concrete walls, corresponding simulations were also carried out at different solar radiation maximums (0–1000 W/m^2). The MPCM concentration and the thickness of concrete samples were kept at 5.2 wt% and 10 cm, respectively. The outdoor temperature, which is based on summer time (July) in Madrid, is described by Eq. (9) with T_{max} = 35 °C, and T_{min} = 15 °C. The indoor surface temperature, the power consumption, power reduction and delay times are summarized in Fig. 4.

As expected, increasing the maximum solar radiation leads to a higher power consumption to maintain an indoor temperature of 23 °C (Fig. 4b). As is evident from Fig. 4b, the power reduction decreases from 29 to 22% when the maximum solar radiation is raised from 0 to 1000 W/m^2. The heat transfer through the wall will increase with more solar radiation, while the MPCM can only absorb a certain amount of heat. During a hot summer, the capacity of the PCM will not be sufficient to compensate for the additional solar radiation. The delay time for the cooling peak decreases from 75 min for 0 W/m^2 to 33 min for 1000 W/m^2 while the heating peak remains approximately stable. This is in good agreement with the indoor surface temperature (Fig. 4a) where the maximum indoor surface temperature increases while the minimum indoor surface temperature remains stable as the maximum solar radiation is raised. This is because the solar radiation is only affecting the samples during the daytime (cooling zone), as illustrated in Fig. 2a.

3.3. Effect of concrete wall thickness

For this work, the thickness of wall was varied from 5 to 15 cm in step of 2.5 cm. The outdoor temperature and the solar radiation were described by Eqs. (9) and (8) with T_{max} = 35 °C, T_{min} = 15 °C and a maximal solar radiation of 750 W/m^2.

The temperature regulating capacity of the walls strongly depends on the combination of wall thickness and the content of MPCM. Fig. 5a and b shows the simulated indoor surface heat flux and indoor surface temperature during a 24 h period for different thicknesses of the MPCM-concrete samples containing 5.2 wt% PS-DVB/RT27. Fig. 5a shows that the indoor surface heat flux decreases as the sample becomes thicker. The decline in indoor surface heat flux is caused by the rate of heat conduction through a sample, which is inversely proportional to the

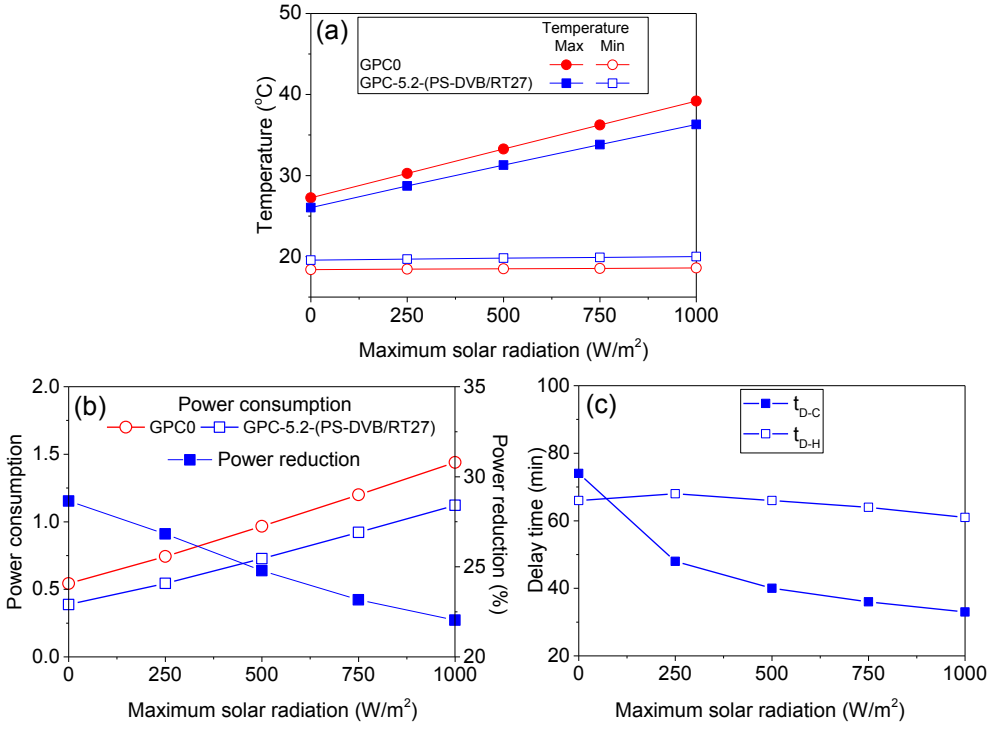

Fig. 4. (a) The maximum and minimum indoor surface temperature; (b) The power consumption of GPC0 and GPC-5.2-(PS-DVB/RT27), and the power reduction of GPC-5.2-(PS-DVB/RT27) compared to GPC0; (c) the delay time of the maximum (t_{D-H}) and minimum (t_{D-C}) power consumption of GPC-5.2-(PS-DVB/RT27) compared to GPC0 as a function of maximum solar radiation.

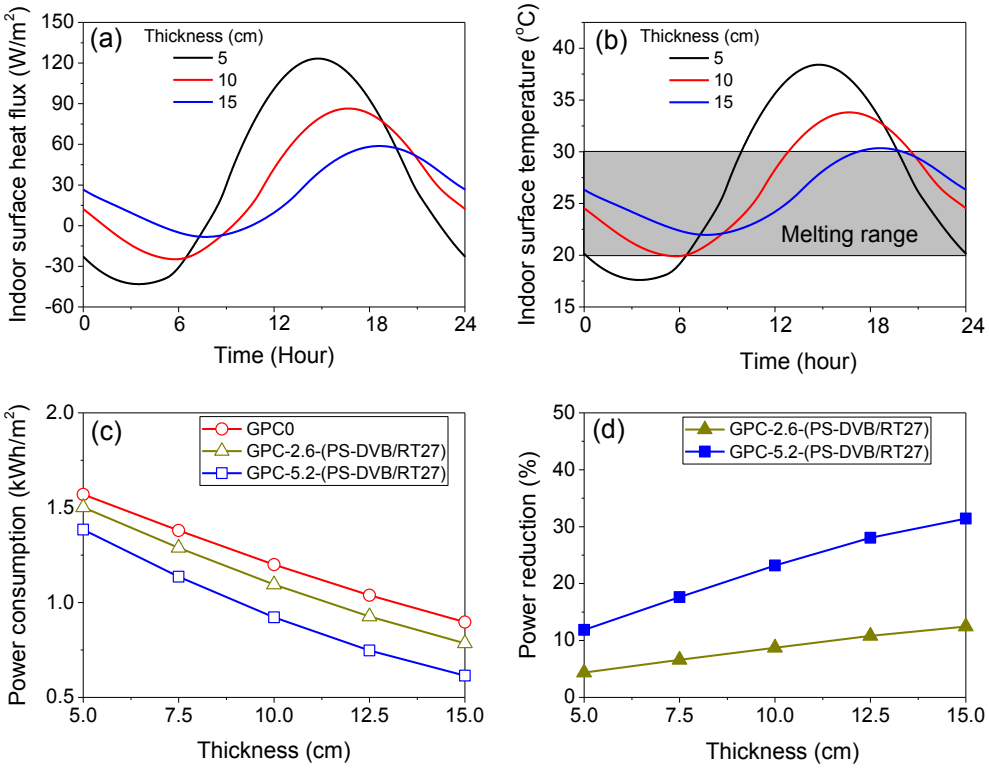

Fig. 5. The effect of thickness on (a) indoor surface heat flux, (b) indoor surface temperature of GPC-5.2-(PS-DVB/RT27), (c) The power consumption and (d) the power reduction of GPC after adding various concentrations of MPCM as a function of concrete thickness.

thickness of the sample (Eq. (6)). The reduced heat transfer through the concrete for the thicker samples combined with the effect of MPCM cause a smaller variation of the indoor surface heat temperature (Fig. 5b) and lower power consumption to maintain the indoor temperature stable at 23 °C (Fig. 5c).

The reduction of power consumption of concrete samples containing different amounts of MPCM compared to corresponding samples without MPCM (GPC0) was calculated as a function of concrete thickness and is illustrated in Fig. 5c. The power reduction increases when the thickness of the sample increases and when the MPCM concentration increases. The cause of the increased efficiency of MPCM addition for the thicker walls can be divulged from Fig. 5b, where it can be seen that the temperature variations of the 15 cm sample covers most of the PCM melting range. This provides good conditions for utilizing the MPCM effect. It is important to point out that although the energy efficiency increases with thicker concrete walls, the thicker walls have higher cost and occupy more housing space.

3.4. Effect of outdoor temperature

In order to find the optimum outdoor environment for utilizing the MPCM concrete as building materials, the relation between different outdoor temperature range variations and the energy efficiency was investigated. In these simulations, the MPCM concentration, concrete thickness and maximum solar radiation were set as 5.2 wt%, 10 cm and 750 W/m^2, respectively. The average outdoor temperature $(T_{max} + T_{min})/2$ was varied from 0 °C to 40 °C while the outdoor temperature amplitude $(T_{max} - T_{min})/2$ was set to 5, 7.5 and 10 °C. The power consumption, power reduction and delay time as a function of the average outdoor temperature are presented in Fig. 6.

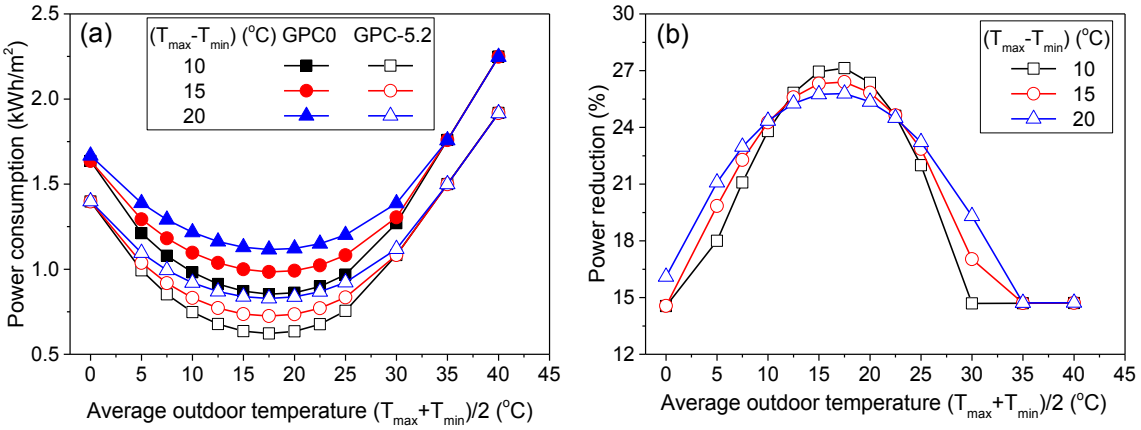

Fig. 6. The effect of average outdoor temperature and the outdoor temperature amplitude on (a) power consumption, (b) power reduction. The thickness of PS-DVB/RT27-concrete wall was 10 cm, and the maximum solar radiation was set at 750 W/m^2.

The power consumption for both GPC0 and GPC-5.2-(PS-DVB/RT27) decreases when the average outdoor temperature is increased, reaching a minimum power consumption when the average outdoor temperature is 15–20 °C, before it increases again at higher temperatures (Fig. 6a). The minimum power consumption is naturally occurring when the average outdoor temperature is close to the desired indoor temperature. The power consumption is much lower when MPCM is added to the concrete, and when the outdoor temperature fluctuations throughout the day is low.

As can be seen from Fig. 6b, the power reduction with the addition of MPCM was about 25–27% at the optimum outdoor temperature average (15–20 °C) for all outdoor temperature amplitudes. At higher or lower outdoor temperature averages, the effect of MPCM is diminished. This demonstrates that MPCM has less effect on the power reduction in extreme cold and hot weather, since the power consumption is strongly dependent on the melting range of MPCM. The efficiency of utilizing MPCM will be higher when the melting range of PCM is fully covered by the temperature variations of walls. Fig. 7 shows the correlation between the indoor and outdoor surface temperature of the concrete and the melting range of the PCM. As can be seen from Fig. 6b, too hot (40 °C) or cold (0 °C) outdoor temperature averages greatly reduce the efficiency of MPCM addition. At these conditions the temperature fluctuations are mostly outside the melting range of the PCM (Fig. 7). It is important to point out that although the effect of phase change is hindered, the reduction of the thermal conductivity of concrete after adding MPCM becomes the dominating effect at these conditions. Interestingly, the power reduction after adding 5.2 wt% PS-DVB/RT27 can reach up to 15% even in extreme hot or cold climate compared to GPC without MPCM.

Furthermore, the power consumption increases while the power reduction decreases as the amplitude of the outdoor temperature oscillations is raised (Fig. 6b). As expected, a broader temperature range require more energy to keep the room temperature stable.

3.5. Evaluation of building envelopes using single wall geopolymer concrete containing MPCM at the climate conditions of Oslo and Madrid

Fig. 8 shows the indoor surface heat flux as a function of time for a south-facing wall over one year at the climate conditions of Oslo and Madrid for GPC without MPCM and GPC containing 5.2 wt% PS-DVB/RT27. The indoor surface heat flux throughout the year is decreased after adding MPCM, leading to a reduced power consumption for the heating and cooling system to maintain the indoor temperature. This is in good agreement with Fig. 3.

The power reduction of concrete samples containing 5.2 wt% MPCM compared to corresponding samples without MPCM (GPC0) for walls facing different directions (south, east, north and west) in Oslo and Madrid during different seasons are presented in Fig. 9. During spring and summer in Oslo, the power reduction for the south and west facing walls are higher than for the walls facing east and north, while all directions are almost the same during autumn and winter. The different solar radiation combined with the outdoor temperature contribute to this effect. Since the outdoor temperature in Oslo is lower than the maintained indoor temperature during most of the year (Fig. 10), the heat provided by solar radiation reduces the heat transfer from the indoor environment toward the outdoor environment. This shifts the indoor wall surface temperature on the south and west walls (which receives most direct sunlight) closer to the indoor temperature (Fig. 10). This effect is most pronounced during spring and summer when the average outdoor temperature is closer to the indoor temperature, and the solar radiation on the south and west facing walls are relatively strong. During autumn and winter (24th September to 20th March), the days are much shorter and the solar radiation is too low to cause significant changes (Fig. 11).

The power reduction in Madrid is highest for the south and west facing walls except during the summer. Unlike Oslo, the solar radiation in Madrid is significant through the whole year (Fig. 11). Interestingly, during summer the power reduction in Madrid is lower for the south and west walls than for the east and north walls. Madrid experiences several summer days with temperatures higher than the indoor temperature. Accordingly, during these periods the added heat from the solar radiation results in a higher power consumption for cooling down the indoor environment.

In order to evaluate the effect of MPM addition on the power consumption of the single house at different seasons during one year in Oslo and Madrid, the average power consumption and power reduction from different wall orientations were calculated (Fig. 12). The power consumption is lowest during the summer and highest during winter in both cities and for all samples. Furthermore, the power reduction is highest in the summer and lowest during winter. The average outdoor temperature during the summer months (15 ± 2 °C in Oslo and 22 ± 2 °C in Madrid) (Fig. 10) is close to the indoor temperature (23 °C) and within the melting range of MPCM, which will improve the efficiency of utilizing the high latent heat of MPCM. The effect of high latent heat during phase change is hindered during winter due to too low temperatures. This is in good agreement with Fig. 6. In addition, the lower power consumption and higher power reduction in Madrid compared to Oslo demonstrates that the utilized MPCM has a higher impact on the warmer climate in Madrid. This is due to an average yearly temperature in Madrid which is closer to the melting range of MPCM (Fig. 10). Accordingly, by adding 5.2 wt% of MPCM to GPC, a single family house in Madrid can reduce the power consumption with up to 24% when utilizing PS-DVB/RT27 and 33% for MF/PCM24 during summer and 16% (PS-DVB/RT27) and 22% (MF/PCM24) during winter (Fig. 12). In Oslo, the power reduction can reach 18% and 24% during summer and 15% and 20% during winter after adding 5.2 wt% of PS-DVB/RT27 and MF/PCM24, respectively. The higher power reduction of concrete containing MF/PCM24 is expected since the heat storage capacity of MF/PCM24 is higher than that of PS-DVB/RT27 (Table 1).

4. Conclusion

A numerical model based on the finite differences method using the energy balance approach was developed to predict the energy saving aspects of buildings utilizing GPC containing 2 types of MPCM at different environmental conditions. Increasing the MPCM concentration and the wall thickness significantly reduce the power consumption and

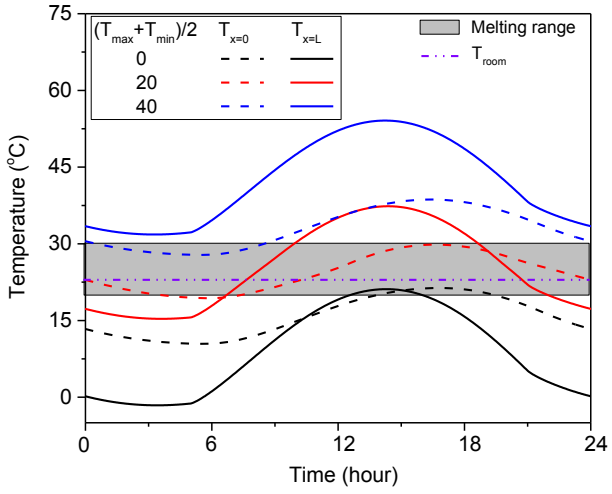

Fig. 7. The correlation between melting temperature range and indoor ($T_{x=0}$) and outdoor surface temperature ($T_{x=L}$) of GPC-5.2-(PS-DVB/RT27) after exposure to average outdoor temperatures of 0, 20, and 40 °C. The amplitude of the outdoor temperature was set to 10 °C, the maximum solar radiation was 750 W/m^2 and the thickness of the concrete wall was 10 cm.

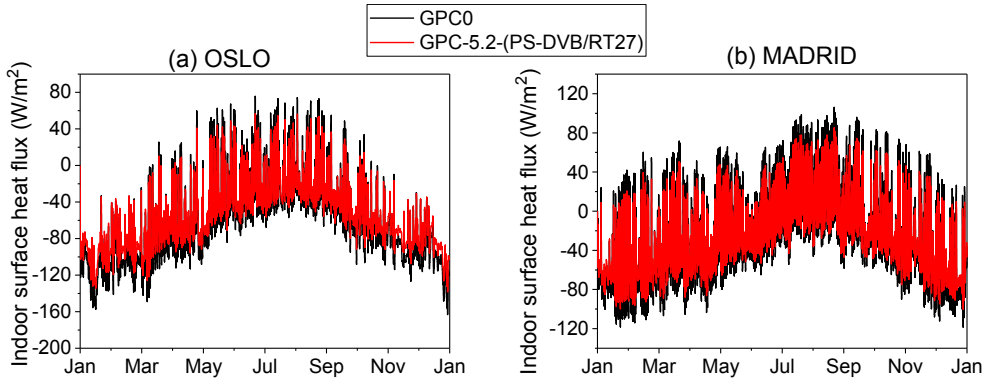

Fig. 8. Indoor surface heat flux as a function of time for a south-facing wall over one year at the climate conditions of (a) Oslo and (b) Madrid for GPC without MPCM and GPC containing 5.2 wt% PS-DVB/RT27.

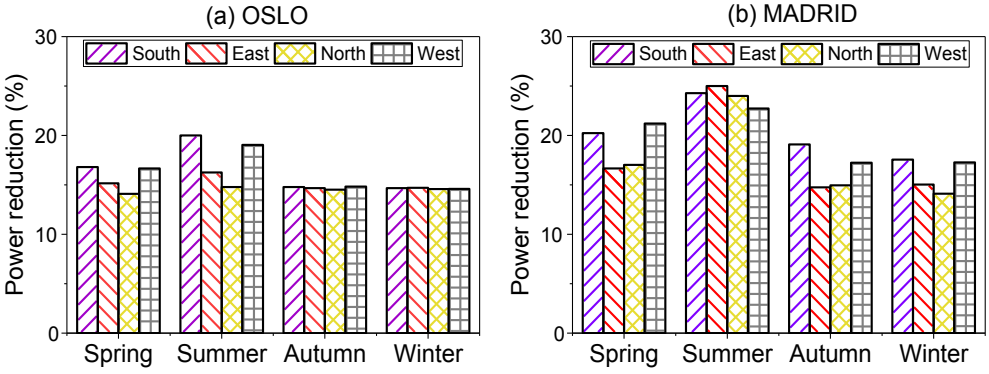

Fig. 9. The power reduction of for South, East, North and West facing walls in Oslo and Madrid utilizing GPC-5.2-(PS-DVB/RT27) compared to GPC0 at different seasons during a year in (a) Oslo and (b) Madrid.

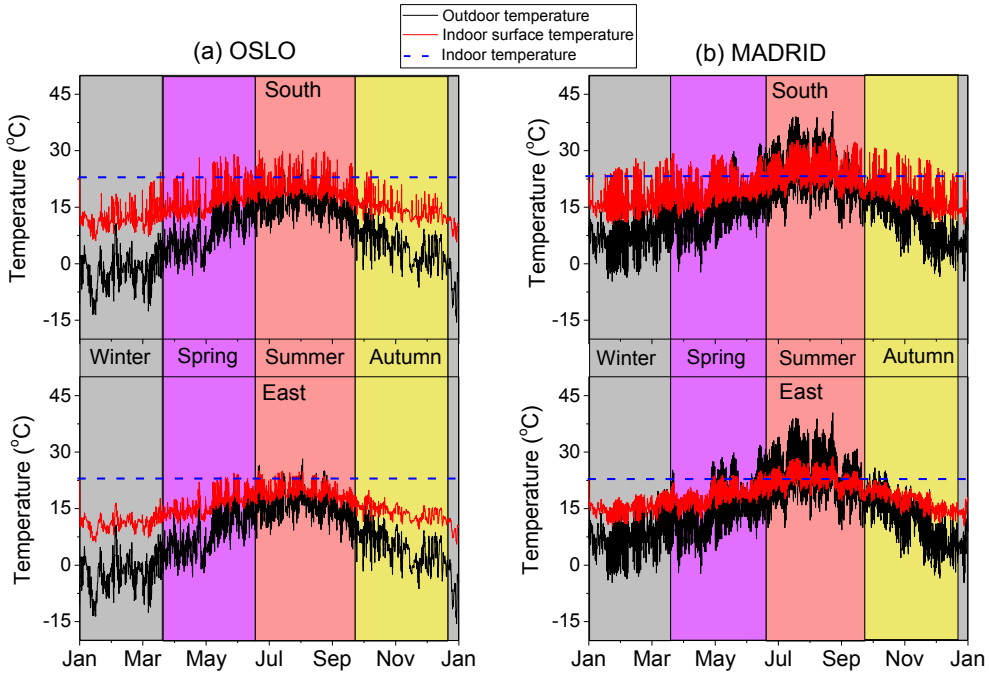

Fig. 10. The outdoor temperature (obtained from weather data-Climate Consultant software (energy-design-tools.aud.ucla.edu.)) and the effect of solar radiation on the indoor surface temperature of the south and east facing walls in (a) Oslo and (b) Madrid.

increase the power reduction of buildings. The energy efficiency of the buildings was reduced at higher levels of solar radiation when the outdoor temperature is higher than the indoor temperature (cooling zone). This illustrates the importance of utilizing a PCM with a melting temperature close to the average outdoor and indoor temperatures, where the effect of the high heat storage capacity during the phase change can be fully utilized. The power reduction with the addition of 5.2 wt% PS-DVB/RT27 was about 25–27% when the average outdoor

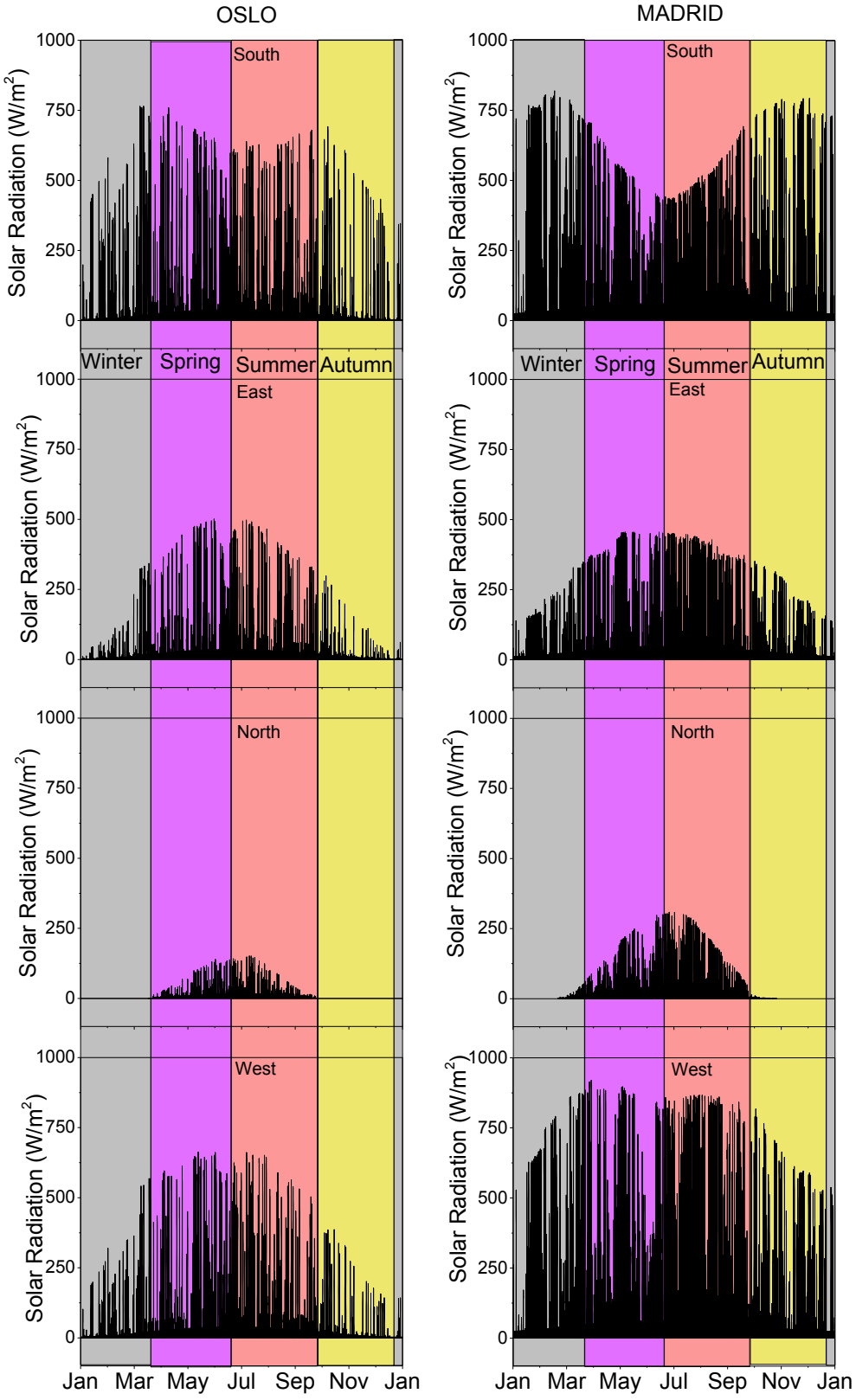

Fig. 11. The solar radiation incident upon a south, east, north and west facing walls as functions of time Oslo and Madrid (obtained from weather data-Climate Consultant software (energy-design-tools.aud.ucla.edu.)).

temperature was15-20 °C for all outdoor temperature amplitudes. Interestingly, the addition of MPCM reduced the power consumption up to 15% even at conditions where the outdoor temperature is extremely warm or cold due to the increased concrete porosity and the resulting lower thermal conductivities.

The numerical model was applied at the conditions of Oslo and Madrid. The annual power reduction was dependent on the orientation of the wall, and was found to be highest for the south and west walls in

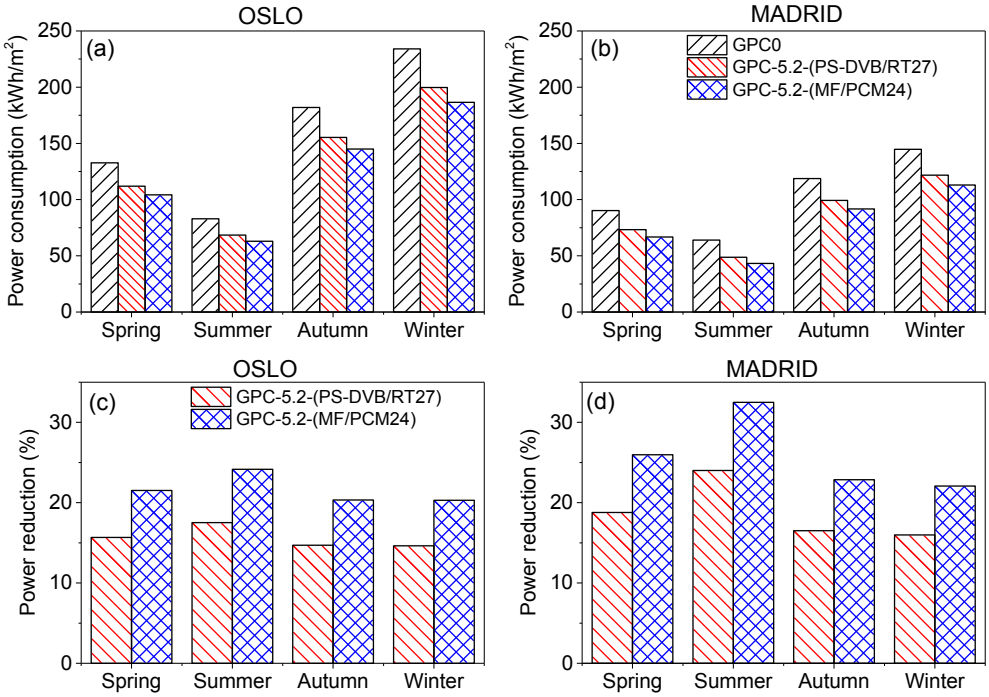

Fig. 12. (a and b) The average power consumption (Eq. (11)) and (c and d) average power reduction (four wall orientations) of utilizing GPC-5.2-(PS-DVB/RT27) and GPC-5.2-(MF/PCM24) compared to GPC0 at different seasons during a year in Oslo and Madrid.

both Oslo and Madrid. The combined effect of solar radiation and outdoor temperature contribute to this effect. The influence of MPCM addition was highest during summer and lowest in winter. This is probably due to that the average outdoor temperature in the summer months (15 ± 2 °C in Oslo and 22 ± 2 °C in Madrid) is close to the indoor temperature (23 °C) and within the melting range of the MPCM. The lower power consumption and higher power reduction of Madrid compared to Oslo is caused by temperatures closer to the melting range of the MPCM. GPC containing MF/PCM24 exhibits a better thermal performance than GPC containing PS-DVB/RT27 due to the higher heat storage capacity and lower thermal conductivity of GPC containing MF/PCM24.

Acknowledgement

We gratefully acknowledge funding from the Research Council of Norway, project number 238198. The authors gratefully acknowledge Rino Nilsen, Trond Atle Drøbak at Østfold University College and Van Thi Ai Nguyen for their assistance with laboratory work.

References

Al-Saadi, S.N., Zhai, Z.J., 2013. Modeling phase change materials embedded in building enclosure: a review. Renew. Sustain. Energy Rev. 21, 659–673.
Al-Sanea, S.A., 2002. Thermal performance of building roof elements. Build. Environ. 37, 665–675.
Alawadhi, E.M., 2008. Thermal analysis of a building brick containing phase change material. Energy Build. 40 (3), 351–357.
Ascione, F., Bianco, N., Masi, R.F.D., Rossi, F.D., Vanoli, G.P., 2014. Energy refurbishment of existing buildings through the use of phase change materials: energy savings and indoor comfort in the cooling season. Appl. Energy 113, 990–1007.
ASHRAE, 2013. Handbook of Fundamentals. American Society of Heating, Refrigerating and Air-Conditioning Engineers. Inc, Atlanta.
Bakharev, T., 2005. Resistance of geopolymer materials to acid attack. Cem. Concr. Res. 35 (4), 658–670.
Benhelal, E., Zahedi, G., Shamsaei, E., Bahadori, A., 2013. Global strategies and potentials to curb CO_2 emissions in cement industry. J. Clean. Prod. 51, 142–161.
Biswas, K., Abhari, R., 2014. Low-cost phase change material as an energy storage medium in building envelopes: experimental and numerical analyses. Energy Convers. Manage. 88, 1020–1031.
Borreguero, A.M., Sánchez, M.L., Valverde, J.L., Carmona, M., Rodríguez, J.F., 2011. Thermal testing and numerical simulation of gypsum wallboards incorporated with different PCMs content. Appl. Energy 88, 930–937.
Borreguero, A.M., Serrano, A., Garrido, I., Rodríguez, J.F., Carmona, M., 2014. Polymeric-SiO_2-PCMs for improving the thermal properties of gypsum applied in energy efficient buildings. Energy Convers. Manage. 87, 138–144.
Cao, V.D., Pilehvar, S., Salas-Bringas, C., Szczotok, A.M., Bui, T.Q., Carmona, M., Rodriguez, J.F., Kjøniksen, A.-L., 2018a. Thermal performance and numerical simulation of geopolymer concrete containing different types of thermoregulating materials for passive building applications. Energy Build. 173, 678–688.
Cao, V.D., Pilehvar, S., Salas-Bringas, C., Szczotok, A.M., Do, N.B.D., Le, H.T., Carmona, M., Rodriguez, J.F., Kjøniksen, A.-L., 2018b. Influence of microcapsule size and shell polarity on the time dependent viscosity of geopolymer paste. Ind. Eng. Chem. Res. 57, 9457–9464.
Cao, V.D., Pilehvar, S., Salas-Bringas, C., Szczotok, A.M., Rodriguez, J.F., Carmona, M., Al-Manasir, N., Kjøniksen, A.-L., 2017. Microencapsulated phase change materials for enhancing the thermal performance of Portland cement concrete and geopolymer concrete for passive building applications. Energy Convers. Manage. 133, 56–66.
Cao, V.D., Pilehvar, S., Salas-Bringas, C., Szczotok, A.M., Valentini, L., Carmona, M., Rodriguez, J.F., Kjøniksen, A.-L., 2018c. Influence of microcapsule size and shell polarity on thermal and mechanical properties of thermoregulating geopolymer concrete for passive building applications. Energy Convers. Manage. 164, 198–209.
Cengel, Y.A., 2002. Heat Transfer: A Practical Approach, second ed. Mcgraw-Hill.
Cui, H., Feng, T., Yang, H., Bao, X., Tang, W., Fu, J., 2018. Experimental study of carbon fiber reinforced alkali-activated slagcomposites with micro-encapsulated PCM for energy storage. Constr. Build. Mater. 161, 442–451.
Cui, H., Liao, W., Mi, X., Lo, T.Y., Chen, D., 2015. Study on functional and mechanical properties of cement mortar with graphite-modified microencapsulated phase-change materials. Energy Build 105, 273–284.
Darkwa, J., Su, O., 2012. Thermal simulation of composite high conductivity laminated microencapsulated phase change material (MEPCM) board. Appl. Energy 95, 246–252.
Diaconu, B.M., Cruceru, M., 2010. Novel concept of composite phase change material wall system for year-round thermal energy savings. Energy Build. 42, 1759–1772.
Eddhahak-Ouni, A., Drissi, S., Colin, J., Neji, J., Care, S., 2014. Experimental and multi-scale analysis of the thermal properties of Portland cement concretes embedded with microencapsulated Phase Change Materials (PCMs). Appl. Therm. Eng. 64 (1–2), 32–39.
EU Directive 2002/91/EC, E.P., Brussels, 2003.
EU Directive 2010/31/UE, E.P., Strasburg, 2010.
Garg, H.P., 1982. Treatise on Solar Energy: Fundamentals of Solar Energy. Wiley, Chichester.
Gowreesunker, B.L., Tassou, S.A., Kolokotroni, M., 2012. Improved simulation of phase change processes in applications where conduction is the dominant heat transfer mode. Energy Build. 47, 353–359.
Hunger, M., Entrop, A.G., Mandilaras, I., Brouwers, H.J.H., Founti, M., 2009. The behavior of self-compacting concrete containing micro-encapsulated Phase Change Materials. Cem. Concr. Comp. 31, 731–743.
Jang, J.G., Lee, N.K., Lee, H.K., 2014. Fresh and hardened properties of alkali-activated

fly ash/slag pastes with superplasticizers. Constr. Build. Mater. 50, 169–176.
Joulin, A., Zalewski, L., Lassue, S., Naji, H., 2014. Experimental investigation of thermal characteristics of a mortar with or without a micro-encapsulated phase change material. Appl. Therm. Eng. 66, 171–180.
Khoshghalb, A., Khalili, N., Selvadurai, A.P.S., 2011. A three-point time discretization technique for parabolic partial differential equations. Int. J. Numer. Anal. Meth. Geomech. 35 (3), 406–418.
Kong, D.L.Y., Sanjayan, J.G., 2010. Effect of elevated temperatures on geopolymer paste, mortar and concrete. Cem. Concr. Res. 40 (2), 334–339.
Kreith, F., Manglik, R.M., Bohn, M.S., 2012. Principles of Heat Transfer, SI ed. Cengage Learning.
Lachheba, M., Karkri, M., Nasrallah, S.B., 2015. Development and thermal characterization of an innovativegypsum-based composite incorporating phase change material asbuilding energy storage system. Energy Build. 107, 93–102.
Lamberg, P., Lehtiniemi, R., Henell, A.-M., 2004. Numerical and experimental investigation of melting and freezing processes in phase change material storage. Int. J. Therm. Sci. 43, 277–287.
Marin, P., Saffari, M., Gracia, A.D., Zhu, X., Farid, M.M., Cabeza, L.F., Ushak, S., 2016. Energy savings due to the use of PCM for relocatable lightweight buildings passive heating and cooling in different weather conditions. Energy Build. 129, 274–283.
Murray Milne, Energy Design Tools: New Non-Residential Energy Tool SBEED 1.0 Released (March, 2017) < http://energy-design-tools.aud.ucla.edu./.
Nematollahi, B., Sanjayan, J., 2014a. Effect of different superplasticizers and activator combinations on workability and strength of fly ash based geopolymer. Mater. Des. 57, 667–672.
Nematollahi, B., Sanjayan, J., 2014b. Efficacy of available superplasticizers on geopolymers. Res. J. Appl. Sci. Eng. Technol. 7, 1278–1282.
Olivia, M., Nikraz, H., 2012. Properties of fly ash geopolymer concrete designed by Taguchi method. Mater. Des. 36, 191–198.
Özişik, M.N., Orlande, H.R.B., Colaço, M.J., Cotta, R.M., 2017. Finite Difference Methods in Heat Transfer. Taylor & Francis Group.
Part, W.K., Ramli, M., Cheah, C.B., 2015. An overview on the influence of various factors on the properties of geopolymer concrete derived from industrial by-products. Constr. Build. Mater. 77, 370–395.
Pasupathy, A., Athanasius, L., Velraj, R., Seeniraj, R.V., 2008. Experimental investigation and numerical simulation analysis on the thermal performance of a building roof incorporating phase change material (PCM) for thermal management. Appl. Therm. Eng. 28, 556–565.
Pérez-Burgos, A., Bilbao, J., Miguel, A.D., Román, R., 2014. Analysis of solar direct irradiance in Spain. Energy Proc. 57, 1070–1076.
Pilehvar, S., Cao, V.D., Szczotok, A.M., Carmona, M., Valentini, L., Lanzón, M., Pamies, R., Kjøniksen, A.-L., 2018. Physical and mechanical properties of fly ash and slag geopolymer concrete containing different types of micro-encapsulated phase change materials. Constr. Build. Mater. 173, 28–39.
Pilehvar, S., Cao, V.D., Szczotok, A.M., Valentini, L., Salvioni, D., Magistri, M., Pamies, R., Kjøniksen, A.-L., 2017a. Mechanical properties and microscale changes of geopolymer concrete and Portland cement concrete containing micro-encapsulated phase change materials. Cem. Concr. Res. 100, 341–349.
Pilehvar, S., Cao, V.D., Szczotok, A.M., Valentini, L., Salvioni, D., Magistri, M., Pamies, R., Kjøniksen, A.-L., 2017b. Mechanical properties and microscale changes of geopolymer concrete and Portland cement concrete containing micro-encapsulated phase change materials. Cem. Concr. Res. 100.
Pisello, A.L., D'Alessandro, A., Fabiani, C., Fiorelli, A.P., Ubertini, F., Cabeza, L.F., Materazzi, A.L., Cotana, Franco, 2017. Multifunctional analysis of innovative PCM-filled concretes. Energy Proc. 111, 81–90.
Ramakrishnan, S., Wang, X., Sanjayan, J., Petinakis, E., Wilson, J., 2017a. Development of thermal energy storage cementitious composites (TESC) containing a novel paraffin/hydrophobic expanded perlite composite phase change material. Sol. Energy 158, 626–635.
Ramakrishnan, S., Wang, X., Sanjayan, J., Wilson, J., 2017b. Assessing the feasibility of integrating form-stable phase change material composites with cementitious composites and prevention of PCM leakage. Mater. Lett. 192, 88–91.
Ramakrishnan, S., Wang, X., Sanjayan, J., Wilson, J., 2017c. Thermal energy storage enhancement of lightweight cement mortars with the application of phase change materials. Proc. Eng. 180, 1170–1177.
Ramakrishnan, S., Wang, X., Sanjayan, J., Wilson, J., 2017d. Thermal performance assessment of phase change material integrated cementitious composites in buildings: experimental and numerical approach. Appl. Energy 207, 654–664.
Ramakrishnan, S., Wang, X., Sanjayan, J., Wilson, J., 2017e. Thermal performance of buildings integrated with phase change materials to reduce heat stress risks during extreme heatwave events. Appl. Energy 194, 410–421.
Sarker, P.K., Kelly, S., Yao, Z., 2014. Effect of fire exposure on cracking, spalling and residual strength of fly ash geopolymer concrete. Mater. Des. 63, 584–592.
Shadnia, R., Zhang, L., Li, P., 2015. Experimental study of geopolymer mortar with incorporated PCM. Constr. Build. Mater. 84, 95–102.
Singh, B., Ishwarya, G., Gupta, M., Bhattacharyya, S., 2015. Geopolymer concrete: a review of some recent developments. Constr. Build. Mater. 85, 78–90.
Sumesh, M., Alengaram, U.J., Jumaat, M.Z., Mo, K.H., Alnahhal, M.F., 2017. Incorporation of nano-materials in cement composite and geopolymer based paste and mortar – a review. Constr. Build. Mater. 148, 62–84.
Szczotok, A.M., Carmona, M., Kjøniksen, A.-L., Rodriguez, J.F., 2017. Equilibrium adsorption of polyvinylpyrrolidone and its role on thermoregulating microcapsules synthesis process. Colloid Polym. Sci. 40, 4061–4071.
Thiele, A.M., Sant, G., Pilon, L., 2015. Diurnal thermal analysis of microencapsulated PCM-concrete composite walls. Energy Convers. Manage. 93, 215–227.
Turner, L.K., Collins, F.G., 2013. Carbon dioxide equivalent (CO_2-e) emissions: a comparison between geopolymer and OPC cement concrete. Constr. Build. Mater. 43, 125–130.
Wei, Z., Falzone, G., Wang, B., Thiele, A., Puerta-Falla, G., Pilon, L., Neithalath, N., Sant, G., 2017. The durability of cementitious composites containing microencapsulated phase change materials. Cem. Concr. Compos. 81, 66–76.
Xie, J., Wang, W., Liu, J., Pan, S., 2018. Thermal performance analysis of PCM wallboards for building application based on numerical simulation. Sol. Energy 162, 533–540.
Zwanzig, S.D., Lian, Y., Brehob, E.G., 2013. Numerical simulation of phase change material composite wallboard in a multi-layered building envelope. Energy Convers. Manage. 69, 27–40.